Comparative degradation study of a biodegradable composite based on polylactide with halloysite nanotubes and a polyacrylic acid copolymer

Comparative degradation study of a biodegradable composite based on polylactide with halloysite nanotubes and a polyacrylic acid copolymer

Petra Drohsler, Muhammad Yasir*, Dalila Rubicela Cruz Fabian, Jaroslav Cisar, Zahra Yadollahi, Vladimir Sedlarik*

Centre of Polymer Systems, University Institute, Tomas Bata University in Zlín, Tr.T. Bati 5678, 76001 Zlín, Czech Republic

* Corresponding authors: M. Yasir (yasir@utb.cz), V. Sedlarik (sedlarik@utb.cz)

Abstract

This study investigates the optimal composition of two additives to accelerate the degradation mechanism of polylactide (PLA) material under different conditions: abiotic hydrolysis, biotic degradation and composting conditions at the laboratory scale level. The composites were prepared from a PLA matrix with a synthesised additive based on a copolymer of polylactic acid and polyacrylic acid (PLA-g-PAA) with inorganic filler halloysite (HNT). The aim was to design a composite material with improved physical and chemical properties and accelerated degradability than conventional PLA, which would apply to products incapable of mechanical or chemical recycling. The addition of HNT alone helped increase Young's modulus by 15 – 25% but worsened the elongation, which was compensated by adding a second additive in the composite. The experimental data from abiotic hydrolysis and biodegradation were processed using appropriate kinetic models. Abiotic hydrolysis was recorded by changes in molecular weights and released carbon (GPC, TOC-L), confirming its acceleration in PLA/5H/20PLA-g-PAA composites by a faster release of ester bonds in PLA. A similar effect was observed during biotic degradation using the measured CO_2 content (GC instrument), which was demonstrated by accelerating from 0.0238 day^{-1} for neat PLA to 0.0397 day^{-1}. In composting conditions, the course was the fastest up to 45 days; samples containing additives were disintegrated by 94.1 – 99.8%, without depreciating the properties of compost and plant germination.

Keywords: accelerated degradation, polylactic acid, composting, biodegradation, abiotic hydrolysis

1. Introduction

Materials based on biodegradable polylactide (PLA) have the great potential to replace the current assortment of polymers, thereby reducing the amount of plastic waste released into the

environment by the industrial and agricultural sectors [1]. Once they have served their practical purpose, items made from such materials are composted with mixed organic waste as a viable means of recovering resources [2,3]. It is necessary that materials of this type disintegrate biologically in composting environments at the same rate as other forms of biodegradable matter, leaving no remnants evident at the end of the process [4].

PLA degrades rapidly in the thermophilic phase of a composting environment, characterised by high temperatures [5,6]. The glass transition temperature for PLA exceeds 58 °C in the process, dramatically accelerating the abiotic hydrolysis. Low-molecular-weight fragments are generated at this stage, constituting a rate-determining step. These are digested and mineralised by microorganisms into essential elements [7]. This phase lasts for a few days, however, compared with the usual course of composting, resulting in insufficient depolymerisation of the chains of the material. The capacity to speed up depolymerisation during composting is prudent, i.e. decreasing the duration required for biodegradation, in order to ensure the material is compatible with surrounding organic by-products.

Several approaches are applicable for treating PLA to promote biodegradation and alter the rate of hydrolysis significantly; examples include copolymerisation and grafting different monomers onto polymer chains [8], blending PLA with extremely biodegradable additives [9,10], or modifying properties, for instance, crystallinity [11,12]. These instances have a significant impact on the rate of deterioration processes. However, such adjustments frequently result in unintended and extensive changes in the desired properties of the material as well, e.g. the thermal resistance and transparency for which PLA is noted [13].

PLA hydrolysis can also be accelerated by boosting ester bond cleavage by utilising an appropriate acid or base. It is known that carboxylic groups in PLA oligomers are able to function as a hydrolysis catalyser [14,15]. However, hydrophilic additives tend to migrate out of the polymer matrix and subsequently exert a significant plasticising effect at larger concentrations. Studies in the literature state that silicates with enough terminal hydroxyl groups have the capacity to enhance abiotic hydrolysis during biodegradation [6,16]. The objective of the research is to discern which biodegradable additive is compatible in this respect and will not alter the properties of the resultant material.

Generally, PLA has certain limitations, for instance, poor thermal, mechanical and barrier resistance [17,18], meaning they are unsuitable for practical use [19]. This makes it necessary to investigate ways of enhancing their characteristics. A recently developed approach is to

fabricate a nanocomposite, a multiphase material made up of two or more parts with continuous and discontinuous phases, e.g. a biopolymer and nanofiller (< 100 nm), respectively [20]. This enhances the properties of the given biopolymer in terms of strength and thermal resistance while also lending the structure stability, as incorporating the nanofiller gives rise to effective interfacial hydrogen bonds between the components. Another advantage of the nanofiller is the low cost, which can reduce the cost of the overall material. Natural biopolymers, metal, metal oxides, and clay are just a few nanofillers referenced in the literature for fabricating nanocomposites [21]. Nanoclay stands out as a good option as it comprises a natural mineral that is harmless, inexpensive and widely utilised commercially [22,23]. If effectively dispersed in the biopolymer matrix, nanoclay also creates an exfoliated structure that improves the desired properties [24].

Halloysite nanotubes (HNTs) constitute a well-known form of nanoclay. HNTs show real potential because they are non-toxic in nature, biocompatible and dispersible [25–27]. They also possess a high cation exchange capacity; thus, a good chance exists of hydrogen bonds forming through the interaction of hydrogen atoms in the PLA with oxygen atoms in the HNTs. This marks the material out as a particularly suitable additive for the biopolymers PLA and PLA-g-PAA (polylactic acid)/poly(acrylic acid). It also disperses well in a matrix, which is crucial in optimising the properties of a nanocomposite film [26].

The concentration of a nanofiller considerably impacts the characteristics of PLA-g-PAA/HNT nanocomposite films, which is why an appropriate amount has to be identified to produce such films with accelerated degradation. Other factors that influence their characteristics are the dispersion of the HNT nanofiller in the PLA, chemical bonds between it and the biopolymer and the average molecular weights of the resultant materials [17,25]. While these discussed the effect of incorporating HNTs on the properties of PLA, the focus remained on specific properties; therefore, a closer, more comprehensive study was required. Indeed, an accelerated degradation experiment involving PLA-g-PAA/HNT nanocomposites has not been published, nor is there analysis of the average molecular weights of such materials [28]. The authors felt that an investigation of these topics was clearly needed to fill the gap in knowledge on effective PLA-g-PAA/HNTs nanocomposite films.

This study aims to develop an optimal composition of a new PLA composite containing natural HNTs in combination with a chemically prepared multi-combed copolymer (PLA-g-PAA) in order to achieve an accelerated PLA degradation process compared to the current state. The weight range of additives in PLA was chosen in this work to clarify the differences between the

samples. The research was carried out first to characterise several concentrations of the composite films to better distinguish their homogenisation and selected properties (mechanical, thermal and wettability) essential for the processing industry. It was believed that the unique chemical structure and the optimal amount of additives would provide PLA material with a higher water-binding ability and help accelerate the hydrolysis of ester bonds. Therefore, the main subject of the research was to monitor the rate of degradation and its course in various environments (abiotic and biotic) with the help of recorded changes (molecular weight, released carbon or carbon dioxide). Kinetic models for degradation processes were also calculated from experimental data. In addition, for possible future applications, disintegration was carried out under composting conditions in laboratory conditions imitating technical composting plants as a possibility of end- life option after their post-use.

2. Materials and Methods

2.1 Materials and Reagents

Commercial PLA (Ingeo 2003D) from NatureWorks (Minnetonka, MN, USA) was utilised in the experiments. Halloysite (HNT) and butylated hydroxytoluene (BHT) were purchased from Sigma-Aldrich, Germany. Tetrahydrofuran (THF) was obtained from Carl Roth Rotisolv® HPLC (Karlsruhe, Germany). The solvents acetone, methanol, acetic acid and ethanol (all analytical grade) were bought from PENTA s.r.o., Prague, Czech Republic. Methanesulphonic acid (MSA, $\geq$ 95%) and poly(acrylic acid) (PAA) 50% solution (M_w = 2000 g·mol^{-1}) were supplied by Sigma Aldrich, Steinheim, Germany.

2.2 Synthesis PLA-g-PAA

The procedure for polymer synthesis adhered to was previously described by Kucharczyk *et al.* [29] as follows: 50 mL L-LA was added into a 250 mL double-necked flask equipped with a Teflon stirrer. The flask was connected to laboratory apparatus for distillation under reduced pressure and placed in an oil bath. Dehydration followed in every instance (160 °C, 200 mBar, 4 h, 180 rpm). Afterwards the reactor was disconnected from the vacuum pump, and the appropriate amount (0.5 wt.%) of MSA and PAA (5 wt.%) were added dropwise under continuous stirring. The pressure was lowered after 1 hour to 20 kPa (165 °C; with an oil pump) and water was distilled out. The pressure was reduced to <1kPa an hour later, upon which the reaction continued for 20 hours. The resulting product was allowed to cool to room temperature

and then dissolved in acetone. The polymer solution obtained was precipitated into a mixture of chilled methanol and distilled water 1:10 (v/v) and filtered. Finally, the product was dried in an oven at 40 °C for 48 hours. The prepolymer was obtained as a white powder, the properties of which are summarised in Table 1.

Table 1
Characterisation of the prepared PLA-g-PAA additive

Sample label	**PAA** (wt.%)	**M_w[a]** ($g \cdot mol^{-1}$)	**Đ[b]** (-)	**T_g** (°C)	**T_m** (°C)
PLA-g-PAA	5	28 000	2.8	52.6	136.2

Where M_w[a] is molecular weight, and Đ[b] is the polydispersity index ($Đ = M_w/M_n$), as determined by Gel Permeation Chromatography (GPC).

2.3 Sample Preparation

The PLA was dried at 60 °C for 24 hours prior to processing. Its neat forms and composites were processed by melt blending on a Brabender mixer (Plastograph® EC plus, Mixer 50EHT32, Duisburg, Germany), and the samples were prepared at the temperature of 190 °C and operating speed of 100 rpm. The mixture obtained from the extruder was cut into small pieces, then pressed into sheets of film at 190 °C for 5 minutes and then cooled. The designation and composition of the prepared samples are detailed in Table 2.

Table 2

Designation and composition of the samples

No. of samples	**PLA** (wt.%)	**HNT** (wt.%)	**PLA-g-PAA** (wt.%)	**Designation**
1	100	-	-	PLA
2	95	5	-	PLA/5H
3	80	20	-	PLA/20H
4	95	-	5	PLA/5PLA-g-PAA
5	80	-	20	PLA/20PLA-g-PAA
6	75	20	5	PLA/20H/5PLA-g-PAA
7	75	5	20	PLA/5H/20PLA-g-PAA

2.4 Characterisation

Conditions for preparing the PLA-g-PAA additive were optimised, involving a direct polycondensation reaction. Several samples of various compositions were fabricated to discern improvement in the behaviour of PLA that had been modified with PLA-g-PAA and supplemented with HNTs. The techniques described below were applied to select the best performing, optimised sample for the accelerated degradation experiment.

2.4.1 Gel Permeation Chromatography (GPC)

GPC analysis was conducted on a PL-GPC 220 chromatographic system (Agilent, Santa Clara, USA), equipped with a dual detection system (a refractive index detector and viscometric detector). The samples were dissolved in THF (2–3 mg×mL^{-1}), stabilised with butylated hydroxytoluene (BHT), and filtered by a syringe filter (0.45 μm). Separation took place on a series of gel-mixed bed columns (Polymer Laboratories Ltd., Amherst, UK) that comprised the following: a PLgel-Mixed-A bed column (300 x 7.8 mm, 20 μm), a PLgel-Mixed-B bed column (300 x 7.8 mm, 10 μm) and a PLgel-Mixed-D bed column (300 x 7.8 mm, 5 μm); the mobile phase contained the THF stabilised with BHT at 40 °C. The flow rate of the mobile phase was set to 1 mL.min^{-1}, and the injection volume equalled 100 μL. The GPC system was calibrated with polystyrene standards for molecular weight within the range of 580–6,000,000 g·mol^{-1} (Polymer Laboratories Ltd., Amherst, UK). The average molar mass or molecular weight (M_w), number average molar mass (M_n) and polydispersity index ($Đ = M_w/M_n$) of the tested samples were determined from peaks corresponding to the polymer fraction, in accordance with the universal calibration method. All data was processed in Cirrus software (Agilent Technologies, Santa Clara, CA, USA).

2.4.2 Scanning Electron Microscopy (SEM)

A Phenom Pro unit (Phenom-World BV, Eindhoven, Netherlands) was used to conduct SEM at an accelerating voltage of 5 kV. Analysis was performed on cryo-fractured portions of the films of neat PLA or composites to evaluate the degree of homogeneity and gain insight into the internal structure of the composites.

2.4.3 Fourier Transform Infrared Spectroscopy

Determining the functional groups present in the thin polymeric films intended for robust degradation testing involved carrying out Fourier transform infrared spectroscopy (FTIR) on a

Nicolet iS5 unit (Thermo Fisher Scientific, Waltham, MA, USA) fitted with a Ge crystal. This took place at ambient temperature, with 64 scans occurring at the resolution of 4 and measurement range of 600–4000 cm^{-1}, with analysis in OMNIC software (Thermo Fisher Scientific, Waltham, MA, USA).

2.4.4 Differential Scanning Calorimetry (DSC)

Thermal properties were investigated on a DSC1 STAR System (Mettler Toledo AG, Greinfensee, Schwerzenbach) under a nitrogen atmosphere (50 $mL \cdot min^{-1}$). A sample of 8–10 mg of each blend was placed in an aluminium pan. The rate of heating and cooling was set to 10 $°C \cdot min^{-1}$, the former of the two ranging from 25 to 180 °C. Values for melting point temperature (T_m), region of glass transition temperature (T_g), melting enthalpy (ΔH_m) and exothermic response relating to cold crystallisation (T_c) were obtained from the first heating cycle.

2.4.5 Thermogravimetric Analysis

Thermogravimetric analysis (TGA) was carried out on equipment by TA Instruments (Wilmington, DE, USA), specifically a TGA Q500 unit and a TA Universal Analyzer 2000, version 4.5A. Samples with an approximate weight of 10 mg were placed in a platinum pan, equilibrated and then heated at temperatures of 25–600 °C at a heating rate of 10 $K \cdot min^{-1}$ in a nitrogen atmosphere at the constant flow rate of 100 $mL \cdot min^{-1}$. A data set was calculated from the percentage of additives remaining in each film after processing them in this manner.

2.4.6 Tensile test

Mechanical properties were investigated on an M350-5 CT universal tensile testing machine (Testometric Company, Lancashire, UK), at a crosshead speed of 10 $mm \cdot min^{-1}$ following the standard ČSN EN ISO 527-1-4. Specimens (of dimension 100 × 10 × 0.5 mm) were cut from the compression moulded films. The samples were stored prior to testing under conditions of 22 °C and 50% relative humidity for 48 hours. A minimum of eight specimens from each group were tested.

2.4.7 Contact angle

Values for the contact angles of the neat PLA and composites were determined on a Surface Energy Evaluation System (SEE System, Advex Instruments, Brno, Czech Republic). A set of seven samples underwent testing for three liquids (water, ethylene glycol and diiodomethane)

in a droplet volume range of 5 µl. The angle was measured approximately a second after the drop had fallen from the micropipette. The free surface energy of the samples was worked out according to the Owen-Went model; the arithmetic averages of five measurements were calculated.

2.5 Abiotic hydrolysis (TOC-L, GPC)

Rates of hydrolysis were gauged for 60 days at 58 °C. In this context, samples of PLA film (50 mg) were cut into 0.5 × 0.5 cm specimens and suspended in 50 ml of sodium phosphate buffer (Na-PB) at (0.1 mol·l^{-1}, pH 7) amended with a microbial growth-inhibiting substance (NaN_3, 0.2% wt.%). The experiment was carried out in triplicates for each sample type, and supernatants were investigated for dissolved organic carbon on a TOC-L Analyser (Shimadzu, Kyoto, Japan). The materials were also evaluated by GPC in parallel at appropriate intervals; three such measurements were taken per sample.

2.6 Biodegradation under composting conditions

The composting test was performed according to ISO 14855-1, applicable for determining the maximum aerobic biodegradability of plastic materials by measuring the amount of carbon dioxide (CO_2) released and the degree of decomposition of the test material at the end of the experiment. The aim was to discern the extent of CO_2 released from the PLA samples placed in a 500 mL reagent bottle equipped with septa mounted on the stoppers. In addition to the sample (50 mg), the bottle contained natural compost (5 g of dry weight) and perlite (5 g). The flasks were incubated at 58 °C for 48 days. Headspace gas was sampled at appropriate intervals through the septum with a gas-tight syringe (100 µL) and then injected manually into an Agilent 7890 GC instrument (Agilent Technologies, Santa Clara, CA, USA), equipped with a Porapak Q (1.829 m length, 80/100 MESH) and 5A molecular sieve (1.829 m length, 60/80 MESH), as well as packed columns connected in series and a thermal conductivity detector (carrier gas helium, flow 53 mL·min^{-1}, column temperature 60 °C). It was possible to calculate the percentage of biodegradation from the data, representing the theoretical amounts of CO_2 produced and oxygen consumed in each flask. From the CO_2 concentration determined, the percentage of mineralisation was calculated pertaining to the carbon content in the initial sample; a TOC-L Analyser was employed for this purpose (SSM-5000A, Shimadzu, Kyoto, Japan).

2.7 Degradation kinetics

Evaluations of data from degradation processes were investigated by applying appropriate kinetic models. The parameters of all individual models were optimised in the MS Excel solver utility program, minimising the sum of squares of residues between the measured data and the interpolated values provided by the models. Their adequacy was compared by the coefficient of determination (R^2). An analytical solution of the proposed model had previously been expressed by Stloukal *et al*. [6].

2.7.1 Hydrolysis

Water-soluble carbon was observed during abiotic hydrolysis by TOC analysis and was recorded at the same time changes in the molecular weight (M_w) of the solid sample. The kinetic model for M_w describes the mechanism of random cleavage during hydrolysis. First-order kinetics were applied to discern M_w; the parameters for the equation, based on the amount of carbon released into the aquatic environment, are given in the supplementary data section (Table S1). Therein, $C_{aq,0}$ (%) is the initial percentage of water-soluble carbon, $C_{h,0}$ (%) represents the initial content of hydrolysable solid carbon, k_{hr} (day^{-1}) denotes the rate constant of first-order hydrolysis for the hydrolysable solid carbon, and c is the duration of the lag phase (days) during the initial phase of biodegradation before the onset of CO_2 production. The rate constant k_{hr} was excluded for mineralisation in an aqueous medium. The parameters for change in M_w in the aquatic environment are detailed in the supplementary data section (Table S2); therein, $M_{w,0}$ ($g \cdot mol^{-1}$) is the average initial weight at time t = 0 and u (day^{-1}) stands for the rate constant of abiotic hydrolysis.

2.7.2 Biodegradation

The kinetic model was adjusted according to the biodegradation conditions and evaluated from the amount of organic carbon released from the solid sample. The related parameters are given in Table 3, wherein $C_{r,0}$ (%) represents the initial content of hydrolysable solid carbon and $C_{aq,0}$ (%) is the initial percentage of water-soluble carbon. The kinetic parameter k_{hr} (day^{-1}) represents the respective rate constant of first-order hydrolysis for the hydrolysable solid carbon; k_{aq} (day^{-1}) expresses the rate constant for the mineralisation (biodegradation) of water-soluble carbon to carbon dioxide; and c is the duration of the delay (days) in the initial phase of biodegradation prior to the commencement of CO_2 production.

2.8 Composting test

The disintegration of samples under composting conditions was performed according to ISO 20200:2004. The plastic reactors were equipped with a composting medium containing 40% sawdust (sourced from a local carpentry business), 30% rabbit feed (Versele-Laga, Deinze, Belgium), 10% ripe compost (Central composting plant, Brno, Czech Republic), 10% corn starch (RUF Lebensmittelwerk KG, Essen, Germany), 5% sugar (Tereos TTD, České Meziříčí, Czech Republic), 4% sunflower oil (Bunge, Chesterfield, MO, USA) and 1% urea (Ing. Petr Švec – PENTA s.r.o., Prague, Czech Republic), which were mixed with water at the ratio of 45:55. Samples were prepared (25 mm x 25 mm, ≤ 5 mm thickness) and buried approximately 2 cm beneath the surface. The reactors (PP boxes, 9.0 x 26.0 x 19.5 cm) were placed in a climatic chamber (Climacell 440, BMT Medical Technology Ltd., Brno, Czech Republic), wherein conditions were set to 58 ± 2 °C and RH 80°. During the 45 days of the test, the reactors were continuously weighed, the pH and temperature inside them were measured and water was added. Reactors were also set aside for GPC sampling and DSC analysis, and photographs were taken. At the close of the test period, the composting media from the reactors were dried and sieved, and the remaining content of polymer residue was subsequently weighed. The ash content of the composting medium, the content of C/N and elements from the leachate were determined by elemental analysis on the TOC-L unit (Shimadzu, Kyoto, Japan) and an EDX device (ARL Quant'X EDXRF spectrometer, Thermo Scientific, Ecublens, Switzerland).

According to the aforementioned standard, the degree of decomposition (*D*) is determined by the percentage of particles trapped on a 2 mm sieve, washed and then dried to constant weight. Loss in weight is expressed according to Equation 1:

$$D(\%) = \left(\frac{m_i - m_r}{m_i}\right) \cdot 100 \quad (1)$$

where m_i corresponds to the initial dry weight of the samples and m_r represents the dry weight of portions of samples obtained by sieving.

The experiment also requires evaluation of the decrease in the volatile solids (R), determined by comparing the actual synthetic waste and the compost obtained at the end, which has to be equal to 30%. R was calculated herein according to Equation 2:

$$R(\%) = \left[\frac{(m_i \cdot DM_i \cdot VS_i) - (m_f \cdot DM_f \cdot VS_f)}{(m_i \cdot DM_i \cdot VS_i)}\right] \cdot 100 \quad (2)$$

Where m_i is the initial mass of the matrix of wet synthetic waste, DM_i is the initial dry mass of the matrix of synthetic waste, and VS_i is the initial volatile-solids content relating to the synthetic waste matrix. M_f, DM_f and VS_f represent the final weight, dry weight and volatile solids of the compost; *DM* and *VS* are expressed as a percentage divided by 100.

Upon completion of the composting test, research on phytotoxicity was also conducted to discern the properties of the compost relating to plant growth and development. A test was performed to calculate the germination index (*IK*), whereby leachate from the compost (1 mL) was dripped on filter paper in a Petri dish (diameter 5 cm) containing watercress seeds (*Lepidium sativum*). Incubation was carried out at 28 °C in the dark over a 24-hours period. Each sample was replicated 10 times for testing purposes (80 seeds in total), including a blank (distilled water). The phytotoxicity test is one of the most widely used methods for biodegradation of the samples in composting practice, adhered to a watercress test devised by the RIAE (Research Institute of Agricultural Engineering in Prague) [30].

$$IK(\%) = 100 \cdot \frac{k_v \cdot l_v}{k_k \cdot l_k} \quad (3)$$

where k_v is the germination of the sample (%), k_k denotes germination of the control (%), l_v stands for the average length of the roots in the sample (mm), and l_k represents the average length of the roots in control (mm).

3. Results and discussion

3.1. Surface morphology of the PLA and modified nanocomposite films

Figure 1 contains SEM images detailing the surfaces and fractured surfaces of the PLA, modified films and HNTs. The surfaces of all the samples are quite similar to one another, varying only in places where either HNT or PLA-g-PAA modification occurred in the PLA matrix. These alterations are more prominent in the fractured cross-sections; for instance, the white particles in Figure 1b′, c′, e′, f′ denote HNT distribution in the structure, as highlighted by the blue arrows. These white spots are absent from Figure 1a′ for neat PLA and Figure 1 d′ and g′ for PLA-g-PAA modification only (without HNT). Despite variance in concentration, HNT had such an affinity with the polymer matrix that the surfaces of the relevant films remained smooth and free of cracks, indicative of homogeneous dispersion in the PLA matrices through significant interaction between the two components. Findings in the literature indicate that positively charged hydrogen atoms of PLA are subject to hydrogen bonding with negatively charged oxygen atoms of HNT. Similarly, hydrogen bonds are also formed between the

siloxane groups in HNT and hydroxyl groups of PLA. Moreover, PLA contains oxygen atoms pertaining to a carboxyl group, which create bonds with hydrogen atoms in the hydroxyl groups of HNT, meaning films of this type possess both thermal stability and enhanced mechanical strength [28].

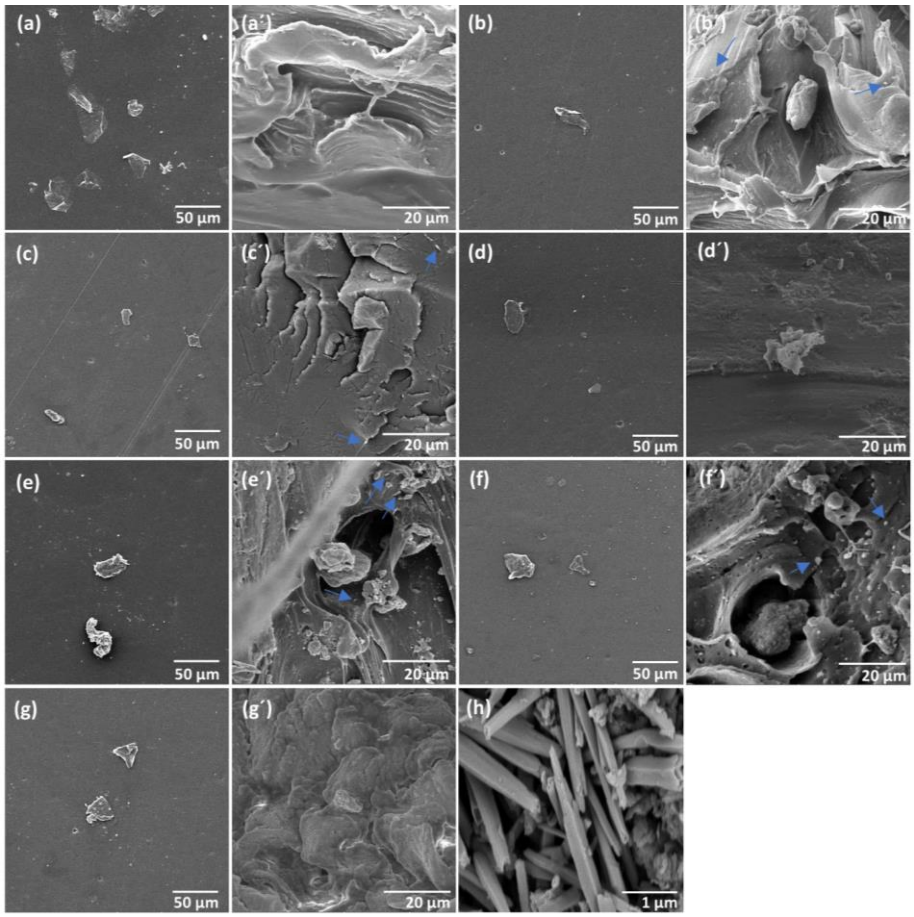

Figure 1. Electron micrographs of the surfaces and fractured surfaces of the thin films: (a, a′) PLA, (b, b′) PLA/5H, (c, c′) PLA/5H/20PLA-g-PAA, (d, d′) PLA/5PLA-g-PAA, (e, e′) PLA/20H, (f, f′) PLA/20H/20PLA-g-PAA, (g, g′) PLA/20PLA-g-PAA and (h) HNTs; (blue arrows indicate HNT particles).

3.2. FTIR spectra for powders of neat PLA, HNT, PLA-g-PAA and the modified films

The FTIR spectra facilitated the identification of the functional groups in the neat PLA, HNT and PLA-g-PAA powders and interactions with the nanocomposite films. The FTIR spectrum for the HNTs demonstrates characteristic peaks at 3695 and 3624 cm^{-1}, indicating a stretching vibration of the O–H bond in the aluminol group, which implies internal and surface stretching, respectively. The peaks at 1029 and 912 cm^{-1} correspond to the symmetrical stretching of the

Si–O–Si bond and bending vibrations of Al–OH, respectively. The peaks observed at 1008 cm^{-1} arise through the absorption/in-plane stretching of Si−O in the HNTs [28]. The slight humps at 1117, 793 and 746 cm^{-1} are caused by in-plane Si−O stretching, Si−O−Si symmetrical stretching and Si−O−Al perpendicular stretching, respectively [31].

The spectra for the PLA-g-PAA powder in Figure 2a and films in Figure 2b resemble the one plotted for neat PLA; however, a broad peak is evident, starting at 1720 cm^{-1} attributed to enhanced −COOH concentration with an increase in the PAA amount. The signals of the PAA, i.e. −CH and $-CH_2$, essentially overlap other signals from that part of the PLA polymer; otherwise, no notable qualitative changes appear in the spectra [32]. Characteristic peaks observed for PLA at 1756, 1269 and 754 cm^{-1} for –C=O relate to its strength vibration, bending vibration and torsion vibration, respectively. The peak located at 955 cm^{-1} corresponds to the C–C group, while the spikes at 1132, 1045 and 869 cm^{-1} belong to C–O groups for strength vibration. The deformation of C−H appears at 1454 cm^{-1}, whereas those expressing symmetrical and asymmetrical strength vibrations of the –CH bond are indicated at 1360 and 1383 cm^{-1}. For the PLA/HNT films, a shift in the lower wavenumber from 1756 to 1752 cm^{-1} for the –C=O bond is visible, owing to strong interactions between the hydroxyl groups of HNT and carbonyl groups of PLA [33]. Adding HNT into the PLA brought about a growth in intensity at 1045 cm^{-1} for the PLA/HNT films, arising through overlap of shifted peaks for HNT at 1029 and 1008 cm^{-1}. The peaks at 869 and 754 cm^{-1} are evidence of the amorphous and crystalline regions present in the PLA, respectively [28].

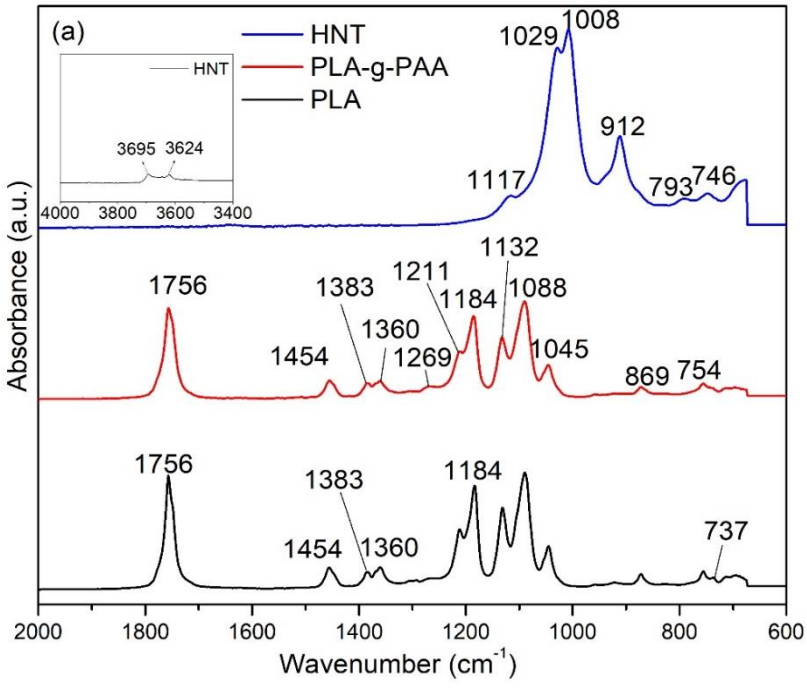

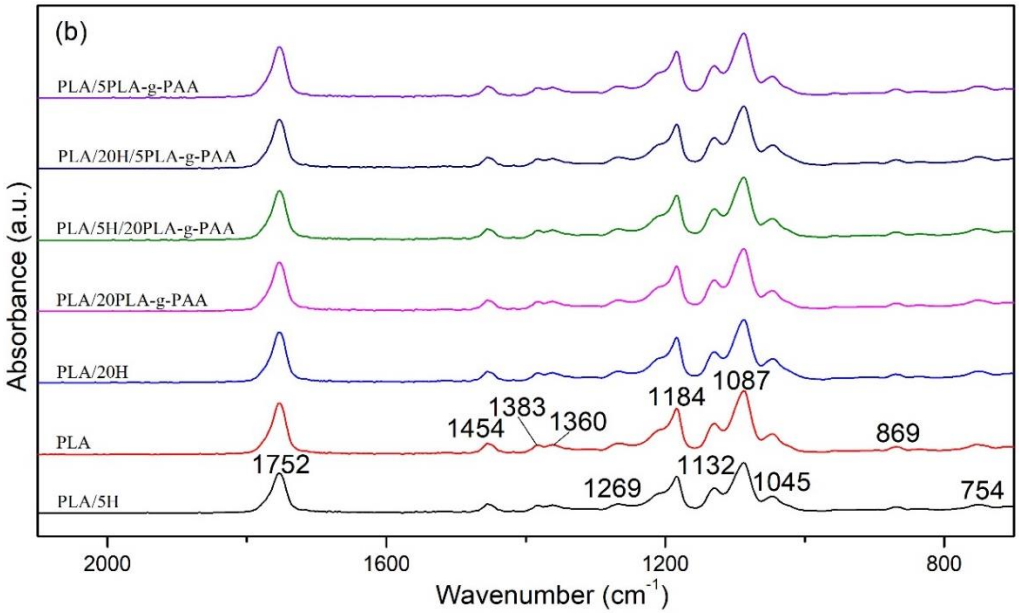

Figure 2. FTIR spectra for attenuated total reflectance (ATR) samples of PLA, PLA-g-PAA and HNT in (a) powdered form and (b) pristine PLA and modified films.

3.3. TGA

The degradation of samples containing both the HNT and PLA-g-PAA additives were compared with neat PLA. Results corresponding to temperatures for onset degradation (T_{onset}) and maximum degradation (T_{max}), as detailed in Table 3, revealed a trend for HNT content. In addition, the TGA and DTGA curves of PLA and their composites were processed from the data, which are part of the set of Appendix Supporting data marked as Figure S1. Not only was T_{onset} affected by increasing HNT concentration, which was lower by up to 8% (in the case of 20 wt.%), but there was also a significant reduction in the degradation maximum by up to 9% (30 °C). The thermal stability of the PLA-g-PAA samples was not significantly affected. In general, HNTs are particles that tend to disperse well in a PLA matrix, and by-products with a net negative charge on their exterior surfaces are known to promote an increase in thermal stability during combustion. A slight decrease in the thermal stability of PLA was witnessed herein, though, potentially caused by HNT agglomerates formed in the mixing process [25,34]. Both of the additives slightly reduced the thermal stability of the PLA, yet most values remained above 292 °C. The thermal effect for samples containing 5% PLA-g-PAA was the lowest observed.

Note: HNT degradation is not reported herein as it was considered irrelevant.

Table 3

Effects of the copolymer and nanofiller on thermal stability

Sample	$\mathbf{T_{onset}}$ (°C)	$\mathbf{T_{max}}$ (°C)	**Mass loss** (%)
PLA	317	350	100
PLA/5H	301	332	94
PLA/20H	293	319	78
PLA/5PLA-g-PAA	313	348	100
PLA/20PLA-g-PAA	311	342	100
PLA/20H/5PLA-g-PAA	298	321	82
PLA/5H/20PLA-g-PAA	299	331	94

3.4. Mechanical testing

Mechanical properties are crucial to determining the practicability of materials for most applications, so they function as an essential indicator in the production, storage, transport and handling. Tensile tests frequently evaluate tensile strength properties, elongation at break and Young's modulus. This study set out to investigate what effects are exerted by the combination of HNT nanotubes and PLA-g-PAA as additives in different concentrations when incorporated in a PLA matrix. In this context, HNT, especially at a higher concentration, significantly influenced each monitored parameter. This was most evident in terms of Young's modulus, since values for it rose in parallel with an increase in the percentage of HNT. In the case of PLA/5H, the value went up by 15%, and sample PLA/20H exceeded neat PLA in this regard by 25%. These values indicated that the films with HNT possessed greater stiffness. An opposite trend was seen for composite with 20% PLA-g-PAA, whereby it was lower (up to 5%) than for neat PLA. The HNT composites exhibited a strong effect in connection with PLA-g-PAA, as values for the modulus were reduced compared with neat PLA or the PLA/HNT composites. This phenomenon could be attributed to PLA-g-PAA (with its shorter chains) and how it was incorporated into the polymer matrix. The consequent reduction in intermolecular binding and greater chain mobility in the polymer matrix heightened the flexibility of the films and contributed to the loss of rigidity [35]. The combination of PLA with a lower concentration of HNT and a higher concentration of PLA-g-PAA in the composite films was advantageous because, in some cases, it could match the values for the neat PLA material, giving it more stability. A higher concentration of HNT filler can also reduce the elongation of PLA, and the

opposite was the case with a lower concentration of PLA-g-PAA. However, there is no visible difference in the variations.

Table 4

Mechanical properties of the neat PLA and PLA composites*

Sample	Young's modulus (MPa) (mean ± SD)	Elongation at break (%) (mean ± SD)	Tensile strength (MPa) (mean ± SD)
PLA	$4\,000 \pm 70^{a}$	1.7 ± 0.1^{a}	$49 \pm 3^{a,c}$
PLA/5H	$4\,600 \pm 130^{b,e}$	$1.4 \pm 0.3^{a,b,d,e}$	$48 \pm 3^{a,c}$
PLA/20H	$5\,000 \pm 120^{c}$	1.1 ± 0.3^{b}	$34 \pm 3^{b,d}$
PLA/5PLA-g-PAA	$3\,900 \pm 120^{a,d}$	2.0 ± 0.3^{c}	51 ± 2^{c}
PLA/20PLA-g-PAA	$3\,800 \pm 100^{d}$	$1.8 \pm 0.2^{a,c}$	$47 \pm 3^{a,c,d}$
PLA/20H/5PLA-g-PAA	$4\,700 \pm 70^{e}$	$1.1 \pm 0.2^{b,d}$	31 ± 2^{d}
PLA/5H/20PLA-g-PAA	$4\,000 \pm 130^{a}$	1.4 ± 0.1^{e}	45 ± 3^{a}

* The mean values followed by the same superscript letters in the same column do not exhibit differences at the 5% significance level according to Tukey's test.

3.5. Contact angles

The mean values with the standard deviation are given in Table 5, and the mean values were processed using Tukey's test and recorded in the upper index in lower case letters. Contact angle measurements revealed that incorporating HNT nanotubes did not significantly affect wettability in the case of water. However, in the case of ethylene glycol, a phenomenon was manifested that was the opposite of expectations, namely that the hydrophobicity of samples containing HNT increased with the increasing content of this filler. This phenomenon could be due to the hydrophobic nature of HNTs with a low number of hydroxyl groups, which led to a decrease in water absorption capacity, or also to the well-dispersed HNTs in the mixed matrices, which could use some free -OH to form hydrogen bonds between them [36]. The surface free energy (SFE) varies with the amount and type of filler added to the PLA matrix. For samples containing PLA-g-PAA, these changes are not striking, but in the case of composites containing 20% HNT, there is a slight increase, which could be caused by a slight agglomeration of this filler in PLA [37]. As confirmed by SEM analysis, every sample was smooth, and cracks were absent that could affect the contact angle.

Table 5

Values for contact angle discerned for liquids (water, ethylene glycol and diiodomethane) and the surfaces of the various samples*

Samples	Contact Angle Values (degrees)			Total SFE ($mJ \cdot m^{-2}$)
	Water	Ethylene glycol	Diiodomethane	
PLA	68 ± 4^{a}	34 ± 6^{a}	42 ± 6^{a}	45 ± 1^{a}
PLA/5H	62 ± 4^{a}	43 ± 4^{b}	37 ± 3^{a}	45 ± 1^{a}
PLA/20H	62 ± 3^{a}	47 ± 4^{b}	37 ± 2^{b}	48 ± 0^{b}
PLA/5PLA-g-PAA	67 ± 3^{a}	41 ± 2^{a}	42 ± 4^{a}	$45 \pm 0^{a,c}$
PLA/20PLA-g-PAA	65 ± 3^{a}	41 ± 1^{a}	40 ± 2^{a}	45 ± 1^{c}
PLA/20H/5PLA-g-PAA	64 ± 3^{a}	47 ± 3^{b}	36 ± 3^{b}	48 ± 0^{b}
PLA/5H/20PLA-g-PAA	60 ± 4^{b}	38 ± 4^{a}	38 ± 2^{a}	45 ± 1^{c}

* Variations are given in parentheses. According to Tukey's tests, samples with different letters are significantly different at 95% confidence interval of probability.

3.6. Abiotic test

The sensitivity of PLA to abiotic hydrolysis is considered an essential factor in determining the applicability of this material from the point of view of durability. Both of the additives (HNT nanotubes and PLA-g-PAA) were added in order to accelerate degradation, even under abiotic conditions. PLA degrades relatively slowly, and the associated process affects abiotic factors, especially temperature and humidity. The hydrolytic behaviour of neat PLA and its composites were observed herein under the influence of abiotic factors, including a high temperature of 58 °C and an aqueous medium (0.1 M Na-PB). Investigation of hydrolysis focused on discerning the content of dissolved organic carbon (TOC-L) and molecular weight (GPC), as illustrated in Figures 3 and 4.

The data collected described the hydrolysis of PLA and its composites as per the carbon released and change in molecular weight in the abiotic environment. Subsequent evaluation was conducted according to the given kinetic models and coefficients of determination (R^2). The kinetic models depicted in the graphs were in good agreement with the experimental data and resultant coefficients, with a level of significance exceeding 0.99. The resulting parameters of the model with R^2 are detailed in the Appendix Supporting data (Table S2).

The hydrolysis experiment revealed that the mineralisation of PLA accelerated due to an increase in the concentration of the PLA-g-PAA additive. Such acceleration was quantified by the length of lag phase *c* calculated from a kinetic model that expressed the initial phase of hydrolysis, i.e., the amount of carbon dissolved in the aqueous medium; this represented a step preceding the final stage of microbial carbon mineralisation during biodegradation. The opposite effect was found for the PLA/HNT composites, primarily those containing 20% HNT. It is known that applying a higher quantity of such nanoparticles could block the release of carboxyl groups from PLA to a certain extent; hence, the rate constants for the hydrolysis increased from 0.041 day^{-1} for neat PLA to approximately 0.058 day^{-1} for PLA supplemented with the PLA-g-PAA additive. Combining both additives in PLA accelerated hydrolysis, a composite containing 5% HNT and 20% PLA-g-PAA stood out in this regard.

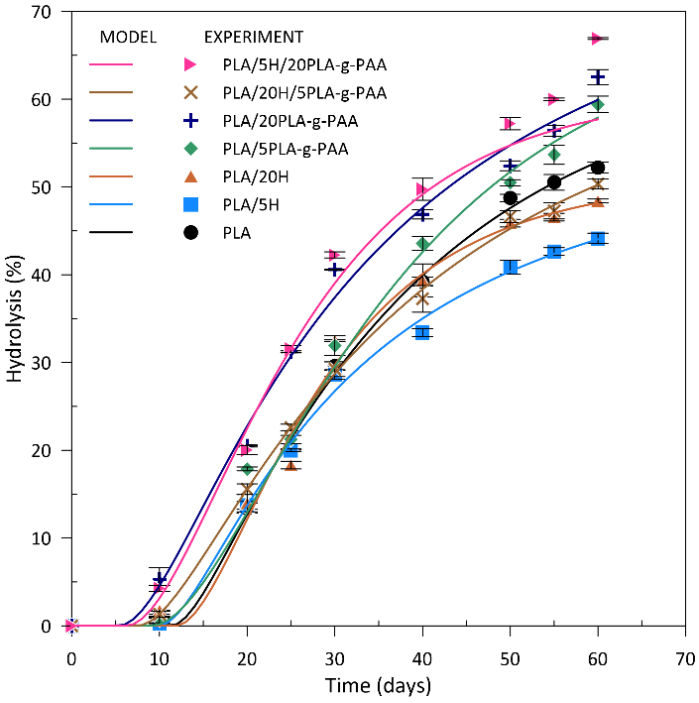

Figure 3. The carbon content of the neat PLA and PLA composites during abiotic hydrolysis in 0.1 M Na-PB (pH~7) at 58 °C.

To learn more about the behaviour of the materials during hydrolysis, they were investigated at the molecular level by GPC. In accordance with loss in molecular weight, findings on the degradation of the neat PLA and composites correlated with previously reported data. Rapid decrease was seen in M_w for neat PLA in the first 10 days, while the presence of PLA-g-PAA heightened the extent of it significantly. The faster onset and course of biodegradation was most likely caused by the PAA, which catalysed the hydrolysis of ester bonds. The molecular weight

of PLA decreased by 76% after 10 days in an abiotic environment (from approximately 201 kg·mol^{-1} to 48 kg·mol^{-1}). The PLA/5PLA-g-PAA and PLA/20PLA-g-PAA samples decreased by 90% (from approximately 170−174 kg·mol^{-1} to 22−11 kg·mol^{-1}), whereas the PLA/5H and PLA/20H composites reduced by 72% from the baseline (from approximately 195−191 kg·mol^{-1} to 49−55 kg·mol^{-1}), respectively. A 99% reduction from their original molecular weight was observed for all the samples after 25 days.

The data obtained were evaluated by first-order kinetics describing for random cleavage of ester bonds; the results are reported in the supplementary data section (Table S2) and illustrated graphically in Figure 3. The rate constants determined for chain cleavage confirmed that the phenomenon was accelerated in PLA supplemented with PLA-g-PAA. The random cleavage of ester bonds in the neat PLA was expressed as a rate constant of 0.1479 days^{-1}, for PLA with PLA-g-PAA ranged from about 0.2056 to 0.2734 days^{-1}. HNT had the opposite effect on hydrolysis, as the rate constant shifted from 0.1430 to 0.1302 day^{-1}.

The results from both analyses confirm the rapid onset and course of degradation by PLA supplemented with PLA-g-PAA, as well as in combination with a limited amount of HNT (5 wt.%). This is highly desirable as its chains degrade rapidly to water-soluble fragments prior to release into the external aqueous medium containing degrading microorganisms. Only from this point can the dissolved oligomers be assimilated and mineralised by the microorganisms in the compost [6].

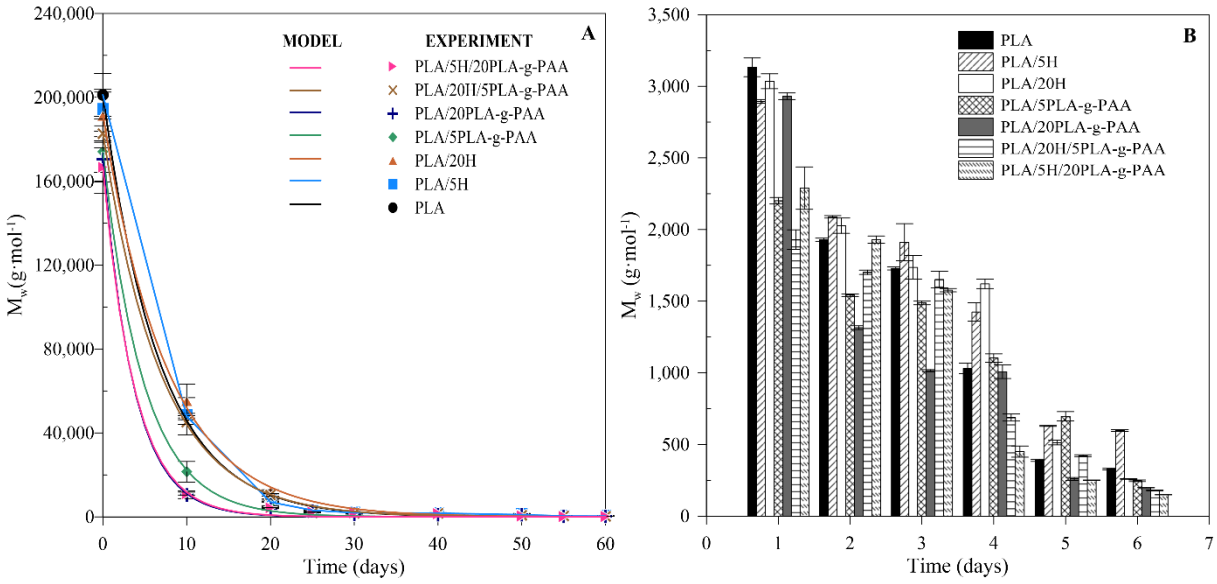

Figure 4. (A) Reduction in molecular weight during abiotic hydrolysis of the neat PLA and various composites with additives according to the kinetic model; (B) the course in the period of 25–60 days according to the measured data is highlighted in the bar graph.

3.7. Biotic degradation test

Aerobic composting (AC) on a laboratory scale made it possible to monitor the biodegradation of the material by gauging the amount of CO_2 released from the test samples [38]. Composting conditions were set at 58 °C after 48 days since control pieces of the cellulose films degraded by more than 70% within 48 days of incubation.

The parameters of the kinetic model and coefficient of determination (R^2) determined from the findings detailed in Figure 5 are presented in the supplementary data section (Table S3). Calculating the kinetic model was performed to predict the course of biodegradation. The values plotted in the graph are in general agreement with the experimental data gathered from all the experiments. The resulting coefficients of determination are notable, with levels of significance exceeding 0.98 for each material.

Every sample under study reached approximately 40% of mineralisation after 48 days of incubation, affirming their biodegradability in the composting medium, although differences between them were observed. The onset of biodegradation was very rapid universally, in contrast to abiotic hydrolysis, which took between 0.3 and 4 days, the most rapid onset being reported for samples containing 20% of the PLA-g-PAA additive. The addition of 5 wt.% HNT in the PLA matrix exerted a positive effect. The samples with PLA-g-PAA showed the fastest onset of mineralisation. The rate constants for biodegradation comprised 0.0238 day^{-1} for PLA, 0.0307 day^{-1} for PLA/5PLA-g-PAA and 0.0364 day^{-1} for PLA/20PLA-g-PAA. The highest value for rate constant (0.0397 day^{-1}) was discerned for the PLA/5H/20PLA-g-PAA composite.

As in the experiment with compost or abiotic hydrolysis, acceleration of PLA hydrolysis tended to occur in samples containing the additive PLA-g-PAA, promoted further through an increase in its concentration. This additive also boosted degradation when in combination with the inorganic filler-HNT. The onset of degradation was faster for all the PLA samples supplemented with HNT and PLA/20PLA-g-PAA than neat PLA. This finding is consistent with reports in the literature on acid-catalysed hydrolysis of PLA ester bonds in the presence of high carboxyl groups, while the structure of HNT also aids water binding and thus accelerates the degradation of PLA [13,29,39].

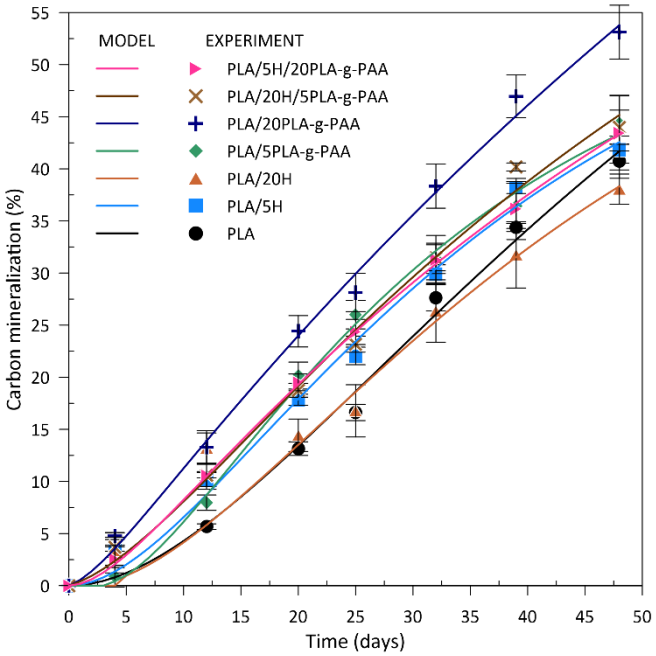

Figure 5. Biodegradation of the PLA, PLA with HNT and PLA-g-PAA/HNT nanocomposite films as converted to carbon content during mineralisation.

3.8. Composting test

Degradation of the samples was observed in terms of change in molecular weight (Figure 6). Samples were taken on day 4, because PLA exhibits quick decomposition from the outset caused by the random and rapid release of its ester bonds, and subsequently at intervals of 7 days. At time 0, molecular weight differed according to the type of additive utilised, and composites with PLA-g-PAA or in combination with HNT demonstrated the lowest values. M_w had reduced by approximately 50% after the first 4 days and by up to 62% for the PLA/20PLA-g-PAA and PLA/5H/20PLA-g-PAA composites. After 7 days, the other composites had degraded by approximately 61%, although the samples containing PLA-g-PAA had decreased by as much as 95%. The expectation had been that HNT would accelerate the degradation of PLA, thanks to bonds that allow faster water binding. The opposite effect by HNT was discerned on molecular weight under composting conditions; however, potentially attributable to a rise in the crystalline phase, in turn retarding degradation.

The molecular weight of all the samples on day 21 equalled ca 3,000 $g \cdot mol^{-1}$, and it was not possible to detect such values after 28 days [39,40].

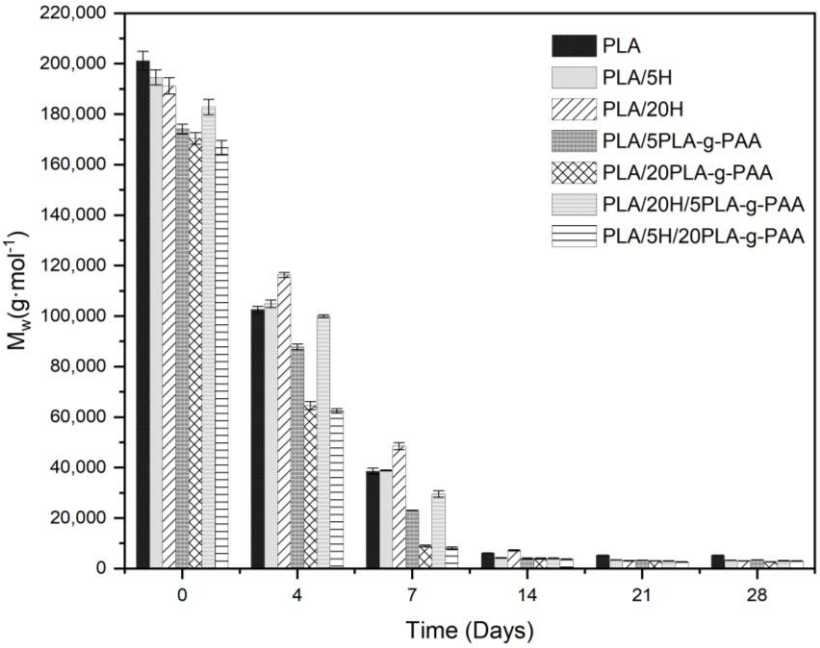

Figure 6. Values for the molecular weight of PLA and PLA composites during degradation under composting conditions.

High molecular weight can slow down the degradation and crystallinity of a polymer. Supplementing PLA with certain additives significantly impacts thermal stability, crystallisation, and thus biodegradation, so DSC analysis was performed to elucidate changes in the behaviour of the polymer and its composites during the composting process [41].

The capacity of PLA is generally relatively poor, and the crystallinity of the films prepared herein was low. When initially exposed to the composting environment, each sample comprised an amorphous polymeric material. Biodegradation under the given composting conditions (58 ± 2 °C and 80% RH) was influenced by various factors, especially temperature and humidity. Temperatures can up to 60 °C in this environment, meaning they align with the range for the glass transition of PLA, thus cold crystallisation occurs in the material. The solubility of PLA is dependent on the molecular weight and degree of crystallinity of the polymer. DSC readings were taken at regular intervals, describing the biodegradation of the neat PLA and composites in the compost. Biodegradation transpired at its fastest rate during the first and second weeks of exposure. The duration of the composting experiment was 45 days, and values for enthalpy of melting (ΔH_m; the content of the crystalline phase in the polymer) are summarised in Table 6.

The temperature in the reactors changed during the test, rising to more than 60 °C, which affected the initial degradation of the samples. This triggered a decrease in molecular weight

alongside increase in melting enthalpies, i.e., crystallinity. Reduction in molecular weight is associated with chains diminishing in length and the formation of lactic acid oligomers that crystallise efficiently [42]. Results compare the PLA to the neat PLA matrix. At the initial stage of degradation (7 days), the PLA/5PLA-g-PAA and PLA/20H/5PLA-g-PAA composites resembled neat PLA. The sample containing the experimentally prepared additive PLA/5PLA-g-PAA was similar in this respect at the end of the test. However, significant differences subsequently emerged in samples containing 20 wt.% of the HNT clay nanotubes, and to a lesser extent in those with 5 wt.% of the same additive. A greater concentration of HNT brought about lower content in the crystalline phase of the polymer composite. The amorphous phase exhibited a high degradation rate for the PLA/20H material [43].

Table 6

DSC results for the neat PLA and composites during degradation under composting conditions.

Sample	**Amorphous materials; after cold crystallisation**		**Crystalline materials**					
	T_g [a] (°C)	**ΔH^b_m** (J/g)	**ΔH^b_m** (J/g)					
	amorphous	crystalline	7 days	14 days	21 days	28 days	35 days	45 days
PLA	65.6	17.5	54.3	84.0	76.5	80.4	75.5	-
PLA/5H	60.4	2.3	39.4	82.6	87.3	77.1	61.1	-
PLA/20H	58.3	12.7	78.4	56.8	47.9	40.3	29.0	-
PLA/5PLA-g-PAA	58.4	34.8	55.9	96.8	88.9	95.2	84.1	-
PLA/20PLA-g-PAA	57.8	3.5	37.6	93.8	84.6	83.2	93.4	-
PLA/20H/5PLA-g-PAA	58.3	13.1	50.1	63.5	60.3	31.0	13.7	-
PLA/5H/20PLA-g-PAA	56.9	30.0	77.0	84.4	68.4	59.5	25.4	-

[a] glass transition temperature determined by DSC.

[b] melting enthalpy determined by DSC (from 1st heating scan) of the studied material.

DSC analysis (Figure 7) also confirmed the effect of the additives on the behaviour of the PLA material, whereby suppressing cold crystallisation in the case of HNT nanotubes. This indicated that the HNT nano clay acted as a nucleating agent for PLA crystallisation [44]. The presence

of PLA-g-PAA was also noticeable in the PLA matrix, manifested by a twofold rise in the melting peak. Differences in biodegradation became more pronounced after 35 days had passed. The PLA samples lost the ability to cold crystallise during the second heating scan, although melting enthalpy increased, indicating that the amorphous parts of the tested samples had biodegraded, leaving merely a crystalline portion. There was also a noticeable loss in melting point associated with chain separation and a reduction in molecular weight for all the samples. Thus, the separation of multiple crystalline chains into semi-crystalline or amorphous portions could have contributed to the microbial degradation of the polymer [45].

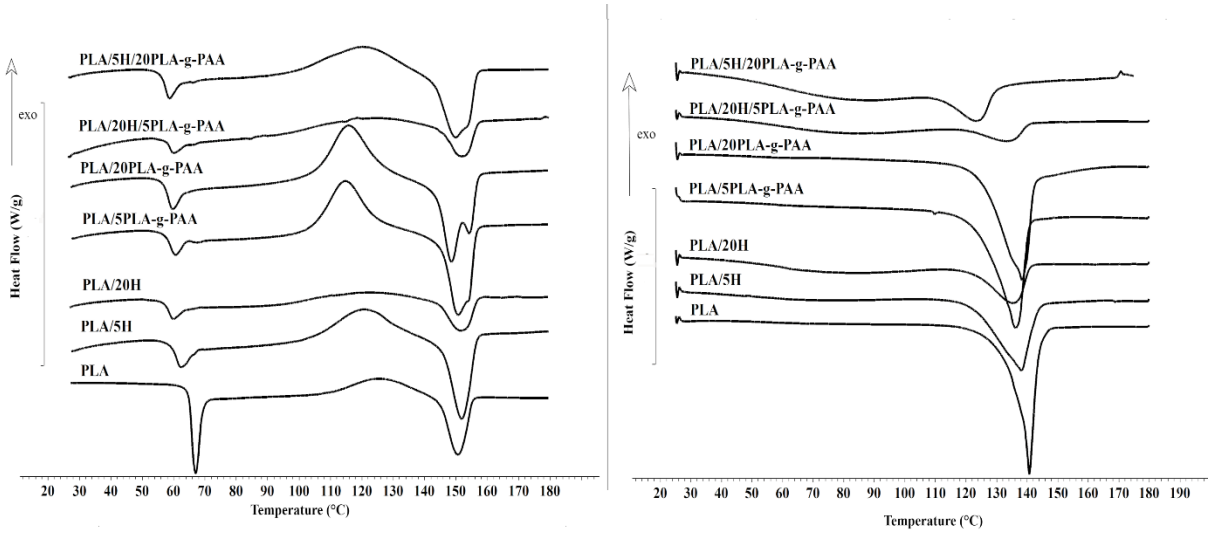

Figure 7. DSC analysis of the neat PLA and PLA composites prior to composting (A) and on day 35 of test (B).

Samples were reported at particular intervals until the end of the composting test at 45 days. Figure 8 shows the changes that occurred to the surfaces of the neat PLA and composites during the composting process in a laboratory setting. Not only did the materials become brittle after 7 days, but an alteration in colour was also evident. In the first phase, yellowing primarily affected the composites with PLA/PLA-g-PAA. An organic segment formed over time, and the samples turned a shade of brown. Those containing up to 20% PLA-g-PAA reached 98% of biodegradation after 45 days, even when they contained 5% HNT. Remnants were visible solely through the presence of the mesh. As for the compost, no residual PLA polymer was discerned after sieving it.

The pH and temperature in the reactors were recorded during the biodegradation experiment. From 0 until day 3, pH equalled 6–8, and the temperature was 58 °C. Then the pH rose sharply to 10–12 and the temperature to 60–62 °C, which remained unchanged until day 10, when both of these gradually decreased; by the 35th day, pH values had dropped to about 9 and the

temperature back to 58 °C. This phase, reported as lasting 3–4 weeks, is referred to as “active”, and the temperature could rise to 70 °C, depending on the material. Compost is hygienized in this phase, whereby pathogenic organisms are destroyed by the high temperature and organic matter is decomposed into basic raw materials. Thermophilic microorganisms at such temperatures facilitate the degradation of complex organic matter, and the conversion of nitrogen to ammonia occurs which raises the pH of the compost. It is possible for the process to end after 35 days, depending on temperature and pH. By this time, a mesophilic phase of polymer degradation has occurred, and fungi are visible to the naked eye. At the end of the composting process it can be assumed that biodegradation has transpired, wherein a decomposing polymer is processed into a humus complex and the compost benefits from a high fertilising effect [46,47].

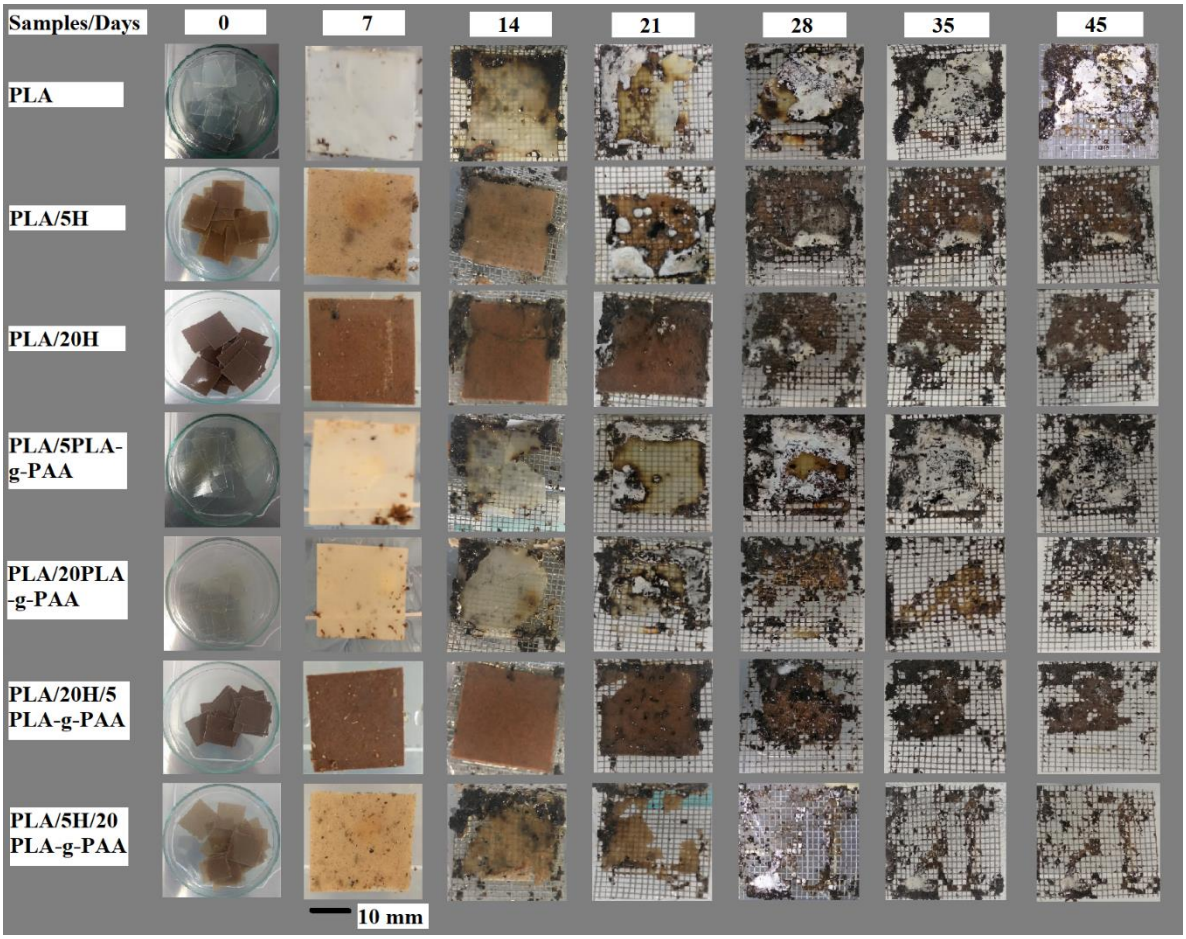

Figure 8. The visual aspect of biodegradation of the neat PLA and PLA composites during the composting experiment.

Approximately 10 g of dried compost was required to prepare the extract. Sampling was performed from each reactor, including a blank. This amount was supplemented with 200 mL

of distilled water, shaken for 24 hours, and then the samples were filtered. An initial quantity of technical waste was prepared for the samples at the beginning of the composting test. The filtered extracts were first analysed from an elemental perspective, revealing changes that occurred during the composting experiment and the possible presence of dangerous or toxic elements. The leachates did not contain hazardous elements, such as As, Cd, Hg, Cu and Pb, i.e., those strictly controlled in drinking water and landfill sites. On the contrary, common elements, including potassium, chlorine and calcium, were found instead (supplementary data section, Table S4). As expected, the chlorine concentration did not differ significantly, ranging at 0.02−0.03 %. The presence of calcium was observed only in minor amounts. The two samples (PLA/5PLA-g-PAA and PLA/20H/5PLA-g-PAA) showed a decrease in potassium, from 0.08% to 0.06–0.04 % [48]. Potassium is an essential nutrient for plants, necessary for their proper development. It is also a positive mobile ion that could interfere with nutrient uptake (fungi) or mineralisation at the concentrations listed here. Each such disruption is followed by stabilisation of it [49].

Table 7 shows the disintegration values for the samples, the percentage of reduction in the volatile matter, the C/N ratio after composting and the results of the phytotoxicity test. The mean values were compared using the Tukey's test with a confidence level of 95% ($p < 0.05$). All of the composted samples degraded by more than 90% in general. Most of the samples were statistically consistent with the neat PLA matrix showing the lowest values, while the PLA/5H/20PLA-g-PAA sample that differed reached almost 100%, as confirmed by Figure 8 above. The content of volatile substances also decreased universally for the samples and blank by more than 70%, indicating that they met the standard requirement, and the end result was higher than 30%. The C/N ratio is a key factor influencing the composting process and related quality. The composting process leads to inevitable losses in nitrogen (N) and carbon (C) through the mineralisation of organic matter by microorganisms, causing the release of dozens of gaseous metabolic products. A C/N ratio of 20–30 is considered optimal for composting. This ratio is often influenced by the composition of the compost, as plant components heighten this ratio while manure and foodstuff residues diminish it. The results revealed that the compost reached a C/N ratio of 8–9, comparable in all cases after 45 days of incubation. The properties of compost are often adjusted by mixing in bulking agents (e.g. straw, leaves, and woody material) [50–53].

After the composting test, the phytotoxicity of the compost was investigated, which is essential for determining its maturity, i.e., the influence it has on the overall growth and development of

plants. Percentages denoting germination indices (*IK*) encompass good compost maturity between 80% and 100%, partially matured at >60% and immature at <60%. The effect on germination of the PLA-bound seeds and their composites after 45 days of composting (a minimal duration) was poor for all the samples including the blank. IK values were gauged at ca 50%, indicative of immature compost, for which the pH remained at ca 9. Therefore, it can be assumed that a longer maturation time after 90 days could improve the properties of the compost, as described in the literature [54–56].

Table 7

Biodegradation of the PLA and PLA nanocomposite materials under composting conditions in reactors*

Samples	***D*** (%)	***R*** (%)	**C/N ratio****	***IK*** (%)
Blank	–	$75.7 \pm 0.7^{a,d}$	8.6 ± 0.2^{a}	48.7 ± 3.2^{a}
PLA	$93.2 \pm 3.8^{a,b.c}$	$73.9 \pm 0.5^{a,b,c}$	8.8 ± 0.8^{a}	54.8 ± 4.0^{a}
PLA/5H	$94.1 \pm 3.9^{a,b.c}$	$74.3 \pm 1.0^{a,b,c,d}$	9.1 ± 0.8^{a}	56.7 ± 5.1^{a}
PLA/20H	97.8 ± 0.3^{b}	$74.9 \pm 0.5^{a,d}$	8.3 ± 1.7^{a}	46.2 ± 3.8^{a}
PLA/5PLA-g-PAA	$94.9 \pm 3.0^{a,b.c}$	$73.5 \pm 0.6^{a,b,c}$	8.1 ± 1.1^{a}	49.3 ± 1.6^{a}
PLA/20PLA-g-PAA	$99.4 \pm 0.9^{b,c}$	$73.4 \pm 0.1^{b,d}$	9.3 ± 0.4^{a}	51.1 ± 3.3^{a}
PLA/20H/5PLA-g-PAA	$96.8 \pm 0.3^{a,b}$	73.1 ± 0.2^{c}	8.3 ± 1.0^{a}	52.4 ± 4.4^{a}
PLA/5H/20PLA-g-PAA	99.8 ± 0.4^{c}	76.0 ± 0.2^{d}	9.3 ± 0.8^{a}	49.6 ± 4.1^{a}

* Mean values were processed using Tukey's test, and different letters in the same column indicate significant differences ($p<0.05$).

D – degree of disintegration according to Equation (1)

R – decrease in the content of volatile solids according to Equation (2)

**results obtained from the TOC-L total organic carbon analyser

IK – germination index according to Equation (3)

4. Conclusions

In this work, the effects of different amounts of homogeneously added additives (HNT and PLA-g-PAA) to PLA at various concentrations (5% and 20% w/w) prepared by thermal extrusion followed by pressing into films were compared, especially on the rate of degradation in different environments. Furthermore, the films were characterised by mechanical (tensile properties), thermal (effect on thermal degradation), wettability and overall homogenisation of additives in PLA (optical method) which is important for processing applications. PLA-g-PAA had a plasticiser property when the HNT filler was added, and it increased the strength and stiffness without any significant effect on the thermal stability of the material. The influence of individual additives and their composites was monitored, the inclusion of which effectively supported the degradation of the PLA material. In the case of abiotic hydrolysis, it was noted that the fast lag phase was achieved with composites containing 20% PLA-g-PAA additive, where the quickest course was achieved by PLA/5H/20PLA-g-PAA composite, reaching disintegration by about 30% in 60 days (compared to neat PLA (TOC-L analysis)). Similar results were obtained for molecular weight disintegration and biotic test where degradation was almost twice faster than pure PLA because the additive containing acrylic acid provide chains with a high concentration of terminal carboxyl groups capable of catalysing the random cleavage of ester bonds in the PLA matrix. In the case of composting, the results of these composites confirmed an accelerating effect on PLA degradation, manifested by almost 100% disintegration in 45 days without adversely affecting the compost properties that could prevent plant germination. The optimally designed combination of both components in the sample led to the desired biodegradation of PLA, especially under conditions ideal for composting plants. The results indicate that the composite could be potentially usable in materials that cannot be fully recycled.

Declaration of competing interests

The authors declare that they have no known competing financial interests or personal relationships that could influence the work reported in this paper.

Acknowledgements

The authors gratefully acknowledge the financial support of the Ministry of Education, Youth and Sports of the Czech Republic (grant no. 8JPL19031), and the Internal Grant Agency of TBU in Zlin (grant no. IGA/CPS/2021/002) and DKRVO (RP/CPS/2022/002) under the financial support of the Ministry of Education, Youth and Sports of the Czech Republic.

References

[1] A. Gregorova, V. Sedlarik, M. Pastorek, H. Jachandra, F. Stelzer, Effect of Compatibilizing Agent on the Properties of Highly Crystalline Composites Based on Poly(lactic acid) and Wood Flour and/or Mica, J. Polym. Environ. 19 (2011) 372–381. https://doi.org/10.1007/s10924-011-0292-6.

[2] G. Kale, R. Auras, S.P. Singh, R. Narayan, Biodegradability of polylactide bottles in real and simulated composting conditions, Polym. Test. 26 (2007) 1049–1061. https://doi.org/10.1016/j.polymertesting.2007.07.006.

[3] R. Pantani, A. Sorrentino, Influence of crystallinity on the biodegradation rate of injection-moulded poly(lactic acid) samples in controlled composting conditions, Polym. Degrad. Stab. 98 (2013) 1089–1096. https://doi.org/10.1016/j.polymdegradstab.2013.01.005.

[4] J.H. Song, R.J. Murphy, R. Narayan, G.B.H. Davies, Biodegradable and compostable alternatives to conventional plastics, Philos. Trans. R. Soc. B Biol. Sci. 364 (2009) 2127–2139. https://doi.org/10.1098/rstb.2008.0289.

[5] P. Stloukal, V. Verney, S. Commereuc, J. Rychly, L. Matisova-Rychlá, V. Pis, M. Koutny, Assessment of the interrelation between photooxidation and biodegradation of selected polyesters after artificial weathering, Chemosphere. 88 (2012) 1214–1219. https://doi.org/10.1016/j.chemosphere.2012.03.072.

[6] P. Stloukal, S. Pekařová, A. Kalendova, H. Mattausch, S. Laske, C. Holzer, L. Chitu, S. Bodner, G. Maier, M. Slouf, M. Koutny, Kinetics and mechanism of the biodegradation of PLA/clay nanocomposites during thermophilic phase of composting process, Waste Manag. 42 (2015) 31–40. https://doi.org/10.1016/j.wasman.2015.04.006.

[7] R.J. Mueller, Biological degradation of synthetic polyesters-Enzymes as potential catalysts for polyester recycling, Process Biochem. 41 (2006) 2124–2128. https://doi.org/10.1016/j.procbio.2006.05.018.

[8] Y. Nakayama, T. Inaba, Y. Toda, R. Tanaka, Z. Cai, T. Shiono, H. Shirahama, C. Tsutsumi, Synthesis and properties of cationic ionomers from poly(ester-urethane)s based on polylactide, J. Polym. Sci. Part A Polym. Chem. 51 (2013) 4423–4428. https://doi.org/10.1002/pola.26857.

[9] F. Masmoudi, A. Bessadok, M. Dammak, M. Jaziri, E. Ammar, Biodegradable packaging materials conception based on starch and polylactic acid (PLA) reinforced with cellulose, Environ. Sci. Pollut. Res. 23 (2016) 20904–20914. https://doi.org/10.1007/s11356-016-7276-y.

[10] R. Lipsa, N. Tudorachi, R.N. Darie-Nita, L. Oprică, C. Vasile, A. Chiriac, Biodegradation of poly(lactic acid) and some of its based systems with Trichoderma viride, Int. J. Biol. Macromol. 88 (2016) 515–526. https://doi.org/10.1016/j.ijbiomac.2016.04.017.

[11] R. Renstad, S. Karlsson, Å. Sandgren, A.C. Albertsson, Influence of processing additives on the degradation of melt-pressed films of poly(ε-caprolactone) and poly(lactic acid), J. Environ. Polym. Degrad. 6 (1998) 209–221. https://doi.org/10.1023/A:1021829816140.

[12] R. Pantani, A. Sorrentino, Influence of crystallinity on the biodegradation rate of injection-moulded poly(lactic acid) samples in controlled composting conditions, Polym. Degrad. Stab. 98 (2013) 1089–1096. https://doi.org/10.1016/j.polymdegradstab.2013.01.005.

[13] H. Shinoda, Y. Asou, T. Kashima, T. Kato, Y. Tseng, T. Yagi, Amphiphilic biodegradable copolymer, poly(aspartic acid-co-lactide): Acceleration of degradation rate and improvement of thermal stability for poly(lactic acid), poly(butylene succinate) and poly(-caprolactone), Polym. Degrad. Stab. 80 (2003) 241–250. https://doi.org/10.1016/S0141-3910(02)00404-4.

[14] S.J. De Jong, E.R. Arias, D.T.S. Rijkers, C.F. Van Nostrum, J.J. Kettenes-Van Den Bosch, W.E. Hennink, New insights into the hydrolytic degradation of poly(lactic acid): Participation of the alcohol terminus, Polymer (Guildf). 42 (2001) 2795–2802. https://doi.org/10.1016/S0032-3861(00)00646-7.

[15] J.R. Rocca-Smith, O. Whyte, C.H. Brachais, D. Champion, F. Piasente, E. Marcuzzo, A. Sensidoni, F. Debeaufort, T. Karbowiak, Beyond Biodegradability of Poly(lactic acid): Physical and Chemical Stability in Humid Environments, ACS Sustain. Chem. Eng. 5 (2017) 2751–2762. https://doi.org/10.1021/acssuschemeng.6b03088.

[16] K. Fukushima, D. Tabuani, M. Dottori, I. Armentano, J.M. Kenny, G. Camino, Effect of temperature and nanoparticle type on hydrolytic degradation of poly(lactic acid) nanocomposites, Polym. Degrad. Stab. 96 (2011) 2120–2129.

https://doi.org/10.1016/j.polymdegradstab.2011.09.018.

[17] S.H. Othman, S.A.M. Edwal, N.P. Risyon, R.K. Basha, R.A. Talib, Water sorption and water permeability properties of edible film made from potato peel waste, Food Sci. Technol. 37 (2017) 63–70. https://doi.org/10.1590/1678-457X.30216.

[18] N. Peelman, P. Ragaert, B. De Meulenaer, D. Adons, R. Peeters, L. Cardon, F. Van Impe, F. Devlieghere, Application of bioplastics for food packaging, Trends Food Sci. Technol. 32 (2013) 128–141. https://doi.org/10.1016/j.tifs.2013.06.003.

[19] J.W. Rhim, H.M. Park, C.S. Ha, Bio-nanocomposites for food packaging applications, Prog. Polym. Sci. 38 (2013) 1629–1652. https://doi.org/10.1016/j.progpolymsci.2013.05.008.

[20] E. Jamróz, P. Kulawik, P. Kopel, The Effect of Nanofillers on the Functional Properties of Biopolymer-Based Films: A Review, Polym. . 11 (2019). https://doi.org/10.3390/polym11040675.

[21] S.H. Othman, Bio-nanocomposite Materials for Food Packaging Applications: Types of Biopolymer and Nano-sized Filler, Agric. Agric. Sci. Procedia. 2 (2014) 296–303. https://doi.org/10.1016/j.aaspro.2014.11.042.

[22] N.P. Risyon, S.H. Othman, R.K. Basha, R.A. Talib, Effect of halloysite nanoclay concentration and addition of glycerol on mechanical properties of bionanocomposite films, Polym. Polym. Compos. 24 (2016) 795–802. https://doi.org/10.1177/096739111602400917.

[23] A.C. Souza, R. Benze, E.S. Ferrão, C. Ditchfield, A.C.V. Coelho, C.C. Tadini, Cassava starch biodegradable films: Influence of glycerol and clay nanoparticles content on tensile and barrier properties and glass transition temperature, LWT - Food Sci. Technol. 46 (2012) 110–117. https://doi.org/10.1016/j.lwt.2011.10.018.

[24] N. Peelman, P. Ragaert, B. De Meulenaer, D. Adons, R. Peeters, L. Cardon, F. Van Impe, F. Devlieghere, Application of bioplastics for food packaging, Trends Food Sci. Technol. 32 (2013) 128–141. https://doi.org/10.1016/j.tifs.2013.06.003.

[25] R.T. De Silva, P. Pasbakhsh, K.L. Goh, S.P. Chai, J. Chen, Synthesis and characterisation of poly (lactic acid)/halloysite bionanocomposite films, J. Compos. Mater. 48 (2014) 3705–3717. https://doi.org/10.1177/0021998313513046.

[26] R. Kamble, M. Ghag, S. Gaikawad, B.K. Panda, Review article halloysite nanotubes and applications : A review, J. Adv. Sci. Res. 3 (2012) 25–29.

[27] M. Liu, S.C. Dudley, Role for the unfolded protein response in heart disease and cardiac arrhythmias, Int. J. Mol. Sci. 17 (2015) 1–10. https://doi.org/10.3390/ijms17010052.

[28] N.P. Risyon, S.H. Othman, R.K. Basha, R.A. Talib, Characterisation of polylactic acid/halloysite nanotubes bionanocomposite films for food packaging, Food Packag. Shelf Life. 23 (2020) 100450. https://doi.org/10.1016/j.fpsl.2019.100450.

[29] P. Kucharczyk, A. Pavelková, P. Stloukal, V. Sedlarík, Degradation behaviour of PLA-based polyesterurethanes under abiotic and biotic environments, Polym. Degrad. Stab. 129 (2016) 222–230. https://doi.org/10.1016/j.polymdegradstab.2016.04.019.

[30] No Titleالبترول, n.d.

[31] S. Kouser, S. Sheik, G.K. Nagaraja, A. Prabhu, K. Prashantha, J.N. D'souza, K.M. Navada, D.J. Manasa, Functionalisation of halloysite nanotube with chitosan reinforced poly (vinyl alcohol) nanocomposites for potential biomedical applications, Int. J. Biol. Macromol. 165 (2020) 1079–1092. https://doi.org/10.1016/j.ijbiomac.2020.09.188.

[32] P. Kucharczyk, J. Zednik, P. Humpolicek, Z. Capakova, V. Sedlarik, Versatile synthesis of comb-shaped poly(lactic acid) copolymers with poly(acrylic acid)-based backbones and carboxylic acid end groups, React. Funct. Polym. 111 (2017) 79–87. https://doi.org/10.1016/j.reactfunctpolym.2016.12.012.

[33] S. Sepahi, M. Kalaee, S. Mazinani, M. Abdouss, S.M. Hosseini, Introducing electrospun polylactic acid incorporating etched halloysite nanotubes as a new nanofibrous web for controlled release of Amoxicillin, J. Nanostructure Chem. 11 (2021) 245–258. https://doi.org/10.1007/s40097-020-00362-w.

[34] Y. Chen, L.M. Geever, J.A. Killion, J.G. Lyons, C.L. Higginbotham, D.M. Devine, Halloysite nanotube reinforced polylactic acid composite, Polym. Compos. 38 (2017) 2166–2173. https://doi.org/10.1002/pc.23794.

[35] P. Jantrawut, T. Chaiwarit, K. Jantanasakulwong, C.H. Brachais, O. Chambin, Effect of plasticiser type on tensile property and in vitro indomethacin release of thin films based on low-methoxyl pectin, Polymers (Basel). 9 (2017). https://doi.org/10.3390/polym9070289.

[36] Z.W. Abdullah, Y. Dong, Biodegradable and water resistant poly(vinyl) alcohol (PVA)/starch (ST)/glycerol (GL)/halloysite nanotube (HNT) nanocomposite films for sustainable food packaging, Front. Mater. 6 (2019). https://doi.org/10.3389/fmats.2019.00058.

[37] J. Sun, J. Shen, S. Chen, M.A. Cooper, H. Fu, D. Wu, Z. Yang, Nanofiller Reinforced Biodegradable PLA/PHA Composites: Current Status and Future Trends, Polym. . 10 (2018). https://doi.org/10.3390/polym10050505.

[38] N.K. Kalita, A. Sarmah, S.M. Bhasney, A. Kalamdhad, V. Katiyar, Demonstrating an ideal compostable plastic using biodegradability kinetics of poly(lactic acid) (PLA) based green biocomposite films under aerobic composting conditions, Environ. Challenges. 3 (2021) 100030. https://doi.org/10.1016/j.envc.2021.100030.

[39] P. Stloukal, P. Kucharczyk, Acceleration of polylactide degradation under biotic and abiotic conditions through utilisation of a new, experimental, highly compatible additive, Polym. Degrad. Stab. 142 (2017) 217–225. https://doi.org/10.1016/j.polymdegradstab.2017.06.024.

[40] D. Czarnecka-Komorowska, K. Bryll, E. Kostecka, M. Tomasik, E. Piesowicz, K. Gawdzińska, The composting of PLA/HNT biodegradable composites as an eco-approach to the sustainability, Bull. Polish Acad. Sci. Tech. Sci. 69 (2021) 1–13. https://doi.org/10.24425/bpasts.2021.136720.

[41] Y. Tokiwa, B.P. Calabia, Biodegradability and biodegradation of poly(lactide), Appl. Microbiol. Biotechnol. 72 (2006) 244–251. https://doi.org/10.1007/s00253-006-0488-1.

[42] A. Quitadamo, V. Massardier, V. Iovine, A. Belhadj, R. Bayard, M. Valente, Effect of cellulosicwaste derived filler on the biodegradation and thermal properties of HDPE and PLA composites, Processes. 7 (2019). https://doi.org/10.3390/pr7100647.

[43] F. Luzi, E. Fortunati, D. Puglia, R. Petrucci, J.M. Kenny, L. Torre, Study of disintegrability in compost and enzymatic degradation of PLA and PLA nanocomposites reinforced with cellulose nanocrystals extracted from Posidonia Oceanica, Polym. Degrad. Stab. 121 (2015) 105–115. https://doi.org/10.1016/j.polymdegradstab.2015.08.016.

[44] G. Ozkoc, S. Kemaloglu, Morphology, biodegradability, mechanical, and thermal properties of nanocomposite films based on PLA and plasticised PLA, J. Appl. Polym.

Sci. 114 (2009) 2481–2487. https://doi.org/10.1002/app.30772.

[45] N.K. Kalita, M.K. Nagar, C. Mudenur, A. Kalamdhad, V. Katiyar, Biodegradation of modified Poly(lactic acid) based biocomposite films under thermophilic composting conditions, Polym. Test. 76 (2019) 522–536. https://doi.org/10.1016/j.polymertesting.2019.02.021.

[46] A.L. Meena, M. Karwal, D. Dutta, R.P. Mishra, Composting: Phases and Factors Responsible for Efficient and Improved Composting, Agric. Food. 3 (2021) 85–90. https://doi.org/10.13140/RG.2.2.13546.95689.

[47] Y. Salama, M. Chennaoui, M. El Amraoui, M. Mountadar, A Review of Compost Produced from Biological Wastes: Sugarcane Industry Waste, Int. J. Food Sci. Biotechnol. 1 (2017) 24. https://doi.org/10.11648/j.ijfsb.20160101.14.

[48] J. Havukainen, J. Hiltunen, L. Puro, M. Horttanainen, Applicability of a field portable X-ray fluorescence for analysing elemental concentration of waste samples, Waste Manag. 83 (2019) 6–13. https://doi.org/10.1016/j.wasman.2018.10.039.

[49] M. Irshad, M. Inoue, M. Shezadi, T. Khan, Faridullah, Ammonium, phosphorus and potassium release from animal manure during composting, J. Food, Agric. Environ. 9 (2011) 629–631.

[50] W.M. Zhang, C.X. Yu, X.J. Wang, L. Hai, Increased abundance of nitrogen transforming bacteria by higher C/N ratio reduces the total losses of N and C in chicken manure and corn stover mix composting, Bioresour. Technol. 297 (2020) 122410. https://doi.org/10.1016/j.biortech.2019.122410.

[51] S. Wu, Z. Shen, C. Yang, Y. Zhou, X. Li, G. Zeng, S. Ai, H. He, Effects of C/N ratio and bulking agent on speciation of Zn and Cu and enzymatic activity during pig manure composting, Int. Biodeterior. Biodegrad. 119 (2017) 429–436. https://doi.org/10.1016/j.ibiod.2016.09.016.

[52] M. Kumar, Y.L. Ou, J.G. Lin, Co-composting of green waste and food waste at low C/N ratio, Waste Manag. 30 (2010) 602–609. https://doi.org/10.1016/j.wasman.2009.11.023.

[53] V. Oreopoulou, W. Russ, Utilisation of by-products and treatment of waste in the food industry, Util. By-Products Treat. Waste Food Ind. (2007) 1–316. https://doi.org/10.1007/978-0-387-35766-9.

[54] C. Castillo, A. Nesic, N. Urra, A. Maldonado, Influence of thermoplasticized starch on physical-chemical properties of new biodegradable carriers intended for forest industry, Int. J. Biol. Macromol. 122 (2019) 924–929. https://doi.org/10.1016/j.ijbiomac.2018.11.026.

[55] F. Ruggero, R. Gori, C. Lubello, Methodologies to assess biodegradation of bioplastics during aerobic composting and anaerobic digestion: A review, Waste Manag. Res. 37 (2019) 959–975. https://doi.org/10.1177/0734242X19854127.

[56] F. Luzi, E. Fortunati, A. Jiménez, D. Puglia, D. Pezzolla, G. Gigliotti, J.M. Kenny, A. Chiralt, L. Torre, Production and characterisation of PLA_PBS biodegradable blends reinforced with cellulose nanocrystals extracted from hemp fibres, Ind. Crops Prod. 93 (2016) 276–289. https://doi.org/10.1016/j.indcrop.2016.01.045.